Original paper

Comparison of two beam angular optimization algorithms guided by automated multicriterial IMRT

Tiago Ventura[a,b,c,*], Humberto Rocha[c,d], Brigida da Costa Ferreira[c,e,f], Joana Dias[c,d], Maria do Carmo Lopes[a,b,c]

[a] *Physics Department of University of Aveiro, Campus Universitário de Santiago, 3810-193 Aveiro, Portugal*
[b] *Medical Physics Department of Instituto Português de Oncologia de Coimbra Francisco Gentil, EPE, Avenida Bissaya Barreto, n° 98, 3000-075 Coimbra, Portugal*
[c] *Institute for Systems Engineering and Computers at Coimbra, Rua Sílvio Lima, 3030-290 Coimbra, Portugal*
[d] *Economy Faculty of University of Coimbra and Centre for Business and Economics Research, Avenida Dr. Dias da Silva, nº 165, 3004-512 Coimbra, Portugal*
[e] *School Health Polytechnic of Porto, Rua Dr. António Bernardino de Almeida, nº 400, 4200-072 Porto, Portugal*
[f] *I3N Physics Department of University of Aveiro, Campus Universitário de Santiago, 3810-193 Aveiro, Portugal*

ARTICLE INFO

ABSTRACT

Purpose: To compare two beam angle optimization (BAO) algorithms for coplanar and non-coplanar geometries in a multicriterial optimization framework.
Methods: 40 nasopharynx patients were selected for this retrospective planning study. IMRT optimized plans were produced by Erasmus-iCycle multicriterial optimization platform. Two different algorithms, based on a discrete and on a continuous exploration of the space search, algorithm *i* and *B* respectively, were used to address BAO. Plan quality evaluation and comparison were performed with SPIDERplan. Statistically significant differences between the plans were also assessed.
Results: For plans using only coplanar incidences, the optimized beam distribution with algorithm *i* is more asymmetric than with algorithm *B*. For non-coplanar beam optimization, larger deviations from coplanarity were obtained with algorithm *i* than with algorithm *B*. Globally, both algorithms presented near equivalent plan quality scores, with algorithm *B* presenting a marginally better performance than algorithm *i*.
Conclusion: Almost all plans presented high quality, profiting from multicriterial and beam angular optimization. Although there were not significant differences when average results over the entire sample were considered, a case-by-case analysis revealed important differences for some patients.

1. Introduction

Intensity-modulated radiation therapy (either static/dynamic IMRT or volumetric modulated arc therapy, VMAT) is becoming the standard technique in radiation therapy. Non-uniform intensity fields from multiple directions are used to generate high conformal dose distributions to the tumour. For the standard approach of IMRT/VMAT treatment planning, the plan objectives are usually described by physical or biological descriptors that are typically incorporated in an objective function that will guide the fluence map optimization (FMO) procedure by scoring the goodness of the plan [1]. Searching methods such as linear least squares [2], gradient descent [3] or simulated annealing [4] are used to compute the intensity pattern that provides the best possible trade-off between conflicting planning goals. A trial-and-error iterative

manual tuning of plan parameters (like weights, objectives or beam angles) may be necessary to achieve an acceptable plan. One important difficulty in this iterative process is the fact that it is not possible to know the impact that changing one given parameter will have in the treatment plan, or what are the interdependencies that exist between the different parameters. This iterative process is thus mainly guided by the empirical knowledge of the planner. Furthermore, it is also not possible to link the parameters' values with the desired clinical planning goals. As a result, it is not possible to guarantee that the trial-and-error optimization process will lead to an optimal plan. This process is also more or less time-consuming depending on the case complexity and mostly on the planner skills [5].

Multi-criteria optimization (MCO) methods come up as a natural option to support the IMRT treatment planning decision making

process. Despite presenting less manual interaction, these methods still require some triggering from the planner to obtain good dose distributions. Multiple objectives, resulting from the goals assigned to targets and normal tissues, are simultaneously maximized (or minimized), instead of a single objective function usually applied for the standard approach of inverse planning. As most of the times it is not possible to find a single feasible solution that is simultaneously the best one for every objective [6,7], a set of optimal plan solutions containing the best possible trade-offs between objectives are presented to the decision maker.

Beam angle selection plays also an important role in IMRT optimization. An appropriate beam angle assembly choice, based on a mathematical criterion rather than on the planner experience or on equidistant coplanar arrangement solutions, may lead to important enhancements in the final plan dose distribution solution [8]. Plan quality improvements can be even more significant if non-coplanar directions are included in the optimization process [9]. The use of non-coplanar beam angles in VMAT was also proposed to combine the benefits of arc therapy, such as short treatment times, with the benefits of noncoplanar IMRT plans, such as improved organ sparing. Selected non-coplanar beam angle directions can be used as anchor points of the arc therapy trajectory [10] which further validate the interest of studying the selection of optimal non-coplanar beam angle incidences. Mathematically, the beam angular optimization (BAO) problem can be described as a highly non-convex multi-modal optimization problem with many local minima [11–13], which ideally requires methods with few computing iterations and able to avoid getting trapped in local minimum. BAO solutions are often non-intuitive, so it is important to use optimization approaches that are reliable considering their capacity of delivering optimal solutions [14].

The BAO problem can be addressed in two different ways. One possibility is to decouple the beam angle selection from the FMO and solve the two problems sequentially. In this case, BAO is driven by geometrical measures (e.g., beam's-eye view metrics) or by methods that require prior knowledge of the problem [8,15]. Although computationally efficient, these methods do not fully account for the interplay of beam angles and beamlet weights and plan solution optimality cannot be fully guaranteed. Another possibility is to simultaneously address BAO and FMO problems. FMO optimal solutions are used to assess the beams set plan quality during the BAO [13]. Two completely different mathematical formulations of the BAO problem can be found in the literature: a combinatorial formulation, where the interval of possible gantry angles, [0°, 360°[, is discretized into evenly spaced angles (e.g. {0°,10°,…,350°} for an angle increment of 10°) and a continuous BAO formulation where all possible gantry angles in the interval [0°, 360°[are considered. For the first approach, a combinatorial search for the best ensemble of beams over a discretized space search defined with all possible beam incidences can be done using heuristic methods [12,13,16–20]. However, as this formulation is considered a nondeterministic polynomial time hard problem [21], alternative combinatorial approaches have also been developed. The iterative BAO methods wherein the beams are iteratively subtracted [22] or added [23,24] to a beam ensemble, decreasing significantly the possible number of combinations, are one the most well-known examples. BAO methods based on the continuous exploration of the solutions search space have been explored as an alternative to the combinatorial BAO, namely using pattern search methods [9,25], or considering a parallel multistart derivative-free optimization framework [9,26].

In the present work, the BAO problem is addressed using two algorithms, one belonging to the discrete combinatorial type [23] and the other to the continuous space search approach optimization class [25]. Both algorithms use the FMO objective function to guide the BAO process and the two problems are simultaneously addressed. The BAO algorithms were compared over a set of 40 nasopharyngeal cancer (NPC) clinical cases. The correspondent IMRT plans were optimized by an automated MCO calculation engine developed by Breedveld et al.

[27]. Coplanar and non-coplanar geometry scenarios and different number of beam incidences in treatment delivery were considered in this retrospective planning study. The plans were assessed and compared using SPIDERplan [28], that evaluates the quality of the dose distribution through an intuitive graphic representation and an associated score function that are based on dose prescription aims.

2. Materials and methods

2.1. Patient data

Forty NPC cases, stages T1 – T4; N1 – N3a/N3b, treated with IMRT were selected for this study. Planning target volumes (PTV) delineation and dose prescriptions were based on the Radiation Therapy Oncology Group and the National Comprehensive Cancer Network guidelines. All cases had simultaneous integrated boost prescription delivered in 33 fractions, 70.0 Gy to the tumour PTV and a dose ranging between 54.0 Gy and 59.4 Gy according to the associated risk disease level to the lymph nodes PTVs. Some patients had one or more adenopathies that were also prescribed with 70.0 Gy. Spinal cord, brainstem, retinas, lens, optical nerves, chiasm, pituitary gland, ears, parotids, oral cavity, temporomandibular joints, mandible, oesophagus, larynx, brain, thyroid and lungs were also contoured by the radiation oncologist, as shown in Figs. S1 and S2 in the Supplementary material. The organs-at-risk (OAR) tolerance doses were established in agreement with the institutional protocol for the nasopharyngeal pathology (the reader is referred to the last column of Table S1 in the Supplementary material).

2.2. Plan generation and optimization

FMO for all plans was handled by Erasmus-iCycle IMRT multi-criterial optimization engine [27]. Guided by a wish-list, containing clinical constraints and prioritized objectives, a constraint-based method, 2pεc method, is used to automatically generate a single Pareto optimal IMRT solution for a given set of beams [27]. Beamlets size are set to 10×10 mm^2 with 30 mm of scatter radius for IMRT optimization and 15 mm for the BAO algorithm implemented within Erasmus iCycle. Dose calculation is performed using a pencil-beam dose algorithm with equivalent path length inhomogeneity corrections and no fluence segmentation is performed during or after multicriterial optimization. The wish-list template built for NPC cases, was previously customized according to the established institutional clinical tolerance criteria using five test cases (Table S2 in the Supplementary material). It contained clinical constraints and prioritized objectives that were divided in two optimization levels, according to the clinical tolerance doses, the proximity between PTVs and OARs and its impact on the dose distribution. This configuration, with a progressive dose optimization structure, is appropriate for complex sites, like the NPC cases. It intends to avoid possible limitations that may arise when a dose value achieved in an OAR with a high priority restricts the optimization of another one with a lower priority. The objectives associated with the PTVs were assigned with the Logarithmic Tumour Control Probability (LTCP) function, which is regulated by a cell sensitivity parameter (α). For this study, an α value of 0.75 was applied to guarantee that at least 98% of the PTV volume receives 95% of the prescription dose (D_p). To allow the minimization of lower prioritized objectives, a LTCP sufficient value of 0.5 was defined. The remaining objectives were defined according to the OAR type. For organs with a serial architecture a maximum dose objective was defined. For parallel architectures a mean dose objective was applied. Also, the dose of non-vital OARs, such as lens, optics, retinas, brain or pituitary gland, was minimized using the generalized Equivalent Uniform Dose (gEUD) function with a value of the tissue-specific parameter that describes the volume effect (a) equal to 12.

2.3. Beam angular optimization

For BAO of coplanar and non-coplanar beam geometries two different methods were tested. Both methods used the optimal FMO value to guide the BAO process and the two problems were jointly solved. The number of beams was defined a priori.

In the first method, developed by Breedveld et al. [23,29] and implemented within Erasmus-iCycle, BAO is integrated in the plan optimization framework, considering a discretization of the search space, i.e. the gantry angle $[0°,360°[$ and the couch angle $[-90°,90°]$ intervals are discretized into equally spaced angles with an angle increment of $5°$. Plan generation is done by iteratively adding into the plan beams with an optimal orientation. For a given beam arrangement, all possible candidates will be combined with the beams already selected for the plan and the candidate beam that achieves the lowest score of the fluence optimization problem is added. New beams will be sequentially added until the maximum number of beams initially defined is reached. The way the iterative BAO algorithm works is described in Algorithm i:

Algorithm i

Initialization

- Define n the number of beams;
- Define $\Theta = \{(\theta_i,) \ i= 1,...,N, \ j= 1,...,M\}$ as the discrete set of possible beam directions;
- Set $x^0 := \{\}$ as the set of best beam directions;
- Set $k := 1$;

Iteration

1. Add each direction of Θ (that does not belong to x^{k-1}), one at a time, to x^{k-1} and compute the optimal FMO value of the corresponding beam direction ensemble;
2. $x^k := \{x^{k-1}, (\theta^k, \phi^k)\}$ where (θ^k, ϕ^k) is the beam direction of Θ that added to the directions of x^{k-1} leads to the best optimal FMO value;
3. $k := k + 1$;
4. If $k \leq n$ return to step 1 for a new iteration.

The second approach, developed by Rocha et al. [25], explores the continuous BAO search space using a pattern search method, meaning that there is no need to do any kind of discretization. These class of methods are directional direct search methods and thus do not require the use of derivatives to minimize the objective function. To assure a more effective search for the best objective function local minimum, a set of points spanning as much as possible the entire search space is defined in a preliminary step of the pattern search optimization. Thus, the objective function values of a set of plans with equally spaced orientations that span the entire beam angle search space are determined. The pattern search optimization is organized around two steps: the search step and the poll step. It starts with the search step where any (global) strategy can be used to improve the best objective function value. In this implementation, minimum Frobenius norm quadratic models were used to perform a search over the whole search space [30]. These quadratic models are based on the beam angle sets already considered. If the corresponding objective value is lower than the best objective function minimum value, the search step was successful, and it is repeated. Otherwise the optimization method proceeds to the poll step, where the current best solution is locally improved using the concept of positive basis. If this step fails to obtain a decrease in the objective function value, the step-size parameter is reduced. If the step-size becomes smaller than the defined limit the process stops, otherwise a new loop of the algorithm is performed starting a new search step. When the maximum number of iterations is reached, the pattern search optimization will stop. BAO using pattern search is described in Algorithm B:

Algorithm B

Initialization

- Define n, the number of beams;
- Choose $x_i \in [0, 360]^n$, $i= 1, ..., N$, the starting beam direction ensembles;
- Compute $f(x_i)$, $i= 1, ..., N$, the optimal FMO value for each of the initial points;
- Set $x_i^* := x_i$, $i= 1, ..., N$, as the best points and $f_i^* := f(x_i^*)$, $i= 1, ..., N$ as the corresponding best optimal FMO values;
- Choose $\alpha_i > 0$, $i= 1, ..., N$, the initial step size and $\alpha_{\min}$ the minimum step size;

Iteration (for each of the active searches)

1. *Search step.* Use a minimum Frobenius norm quadratic model considering the beam angle sets already tested to search the entire BAO space. If the objective function value is improved, repeat the search step, otherwise proceed to the poll step.
2. Poll step. Compute $f(x)$, $\forall \ x \in N(x_i^*) = \{x_i^* \pm \alpha_i e_j, j = 1,...,n\}$, where e_j is the j column of identity matrix $I = [e_1...e_n]$;
3. If poll is successful, i.e. $\min_{N(x_i^*)} f(x) < f(x_i^*)$ then

$$x_i^* := \operatorname*{argmin}_{N(x_i^*)} f(x);$$
$$f_i^* := f(x_i^*);$$
Else
$$\alpha_i := \frac{\alpha_i}{2};$$

4. If $\alpha_i \geq \alpha_{\min}$ return to step 1 for a new iteration, otherwise search started by initial point x_i becomes inactive;

Output

- $f^* := \operatorname{argmin} f_i^*$ is the best FMO found and x^* is the corresponding beam direction ensemble.

2.4. Study design

IMRT plans were automatically generated in iCycle for all NPC cases. Based on the defined wish-list, plan optimization was performed using 7 coplanar equidistant beams (*d7*) corresponding to the standard clinical option. In a second phase, plan optimization was done by applying beam angular optimization. Breedveld et al. [23] (algorithm *i*) and Rocha et al. [25] (algorithm B) beam angular optimization algorithms were used to generate IMRT plans with 5, 7 and 9 beams (*i5*, *i7*, *i9* and *B5*, *B7*, *B9*, respectively). For both algorithms, coplanar and non-coplanar beam geometries were considered. For the non-coplanar case it is important to guarantee that there are no collisions between the gantry and the treatment couch (Fig. S3 in the Supplementary material). For algorithm *B*, this is usually achieved by strongly penalizing these solutions (assigning a very large value for the FMO). This means that these solutions can be found in the algorithms' search procedures but will be discarded since better solutions will be found. For algorithm *i*, a space search is defined before the beginning of the optimization that should avoid collisions. However, due to the discretization of the space search, it is not possible to completely prevent beam incidences located in regions defined as avoidable.

2.5. Plan assessment and comparison

Plan assessment and comparison were performed using an independent graphical method developed by Ventura et al. [28]. SPIDERplan, is based on a scoring approach that considers both target coverage and individual OAR sparing. In SPIDERplan framework, targets and OARs are divided into groups depending on their clinical priorities. A score is determined for each structure based on pre-defined planning objectives and relative weights. A global plan score is determined as a weighted sum of the structures' individual scores over all

Table 1

Gantry and couch regions defined for the beam angular distribution analysis. The gantry regions were applied for the coplanar and non-coplanar analysis (circular diagrams and 2D-maps, respectively) and the couch regions to the non-coplanar analysis.

Gantry		Couch	
Region label	Angle region	Region label	Angle region
Anterior	[340°, 20°[	Left coronal (LCOR)	[−90°, −70°[
Left oblique anterior (LOA)	[20°, 70°[	Oblique left non-coplanar (OLNC)	[−70°, −20°[
Left lateral (LL)	[70°, 110°[	Central non-coplanar (CNC)	[−20°, 20°[
Left oblique posterior (LOP)	[110°, 160°[	Oblique right non-coplanar (ORNC)	[20, 70°[
Posterior	[160°, 200°[	Right coronal (RCOR)	[70, 90°]
Right oblique posterior (ROP)	[200°, 250°[		
Right lateral (RL)	[250°, 290°[		
Right oblique anterior (ROA)	[290°, 340°[		

groups. This score is just a quality plan indicator without any direct correlation with the treatment outcome. All dosimetric plan information is graphically represented in customized radar plots. Evaluation of plan quality can be done globally by displaying all structures (Structures Plan Diagram – SPD) and groups of structures (Group Plan Diagram – GPD). Global plan score is determined as a weighted sum of the structures individual scores over all groups as:

$$\text{Global plan score} = \sum_i w_{group(i)} \sum_j w_{struct(j)} \text{Score}_{struct(j)} \qquad (1)$$

where $w_{struct(j)}$ and $\text{Score}_{struct(j)}$ are the relative weight and the score of structure j, respectively, and $w_{group(i)}$ the relative weight of group i. For the PTVs, the score was calculated according to the following expression:

$$\text{Score}_{PTV} = \frac{D_{TC,PTV}}{D_{P,PTV}} \qquad (2)$$

where $D_{TC,PTV}$ corresponds to the tolerance criteria for the PTV (in this case the dose in 98% of the PTV that should be at least 95% of the prescribed dose, Table S1) and $D_{P,PTV}$ is the planned dose in the PTV. This is a target coverage criterion. For the OARs, the score was set as:

$$\text{Score}_{OAR} = \frac{D_{P,OAR}}{D_{TC,OAR}} \qquad (3)$$

where $D_{P,OAR}$ is the OAR planned dose and $D_{TC,OAR}$ is the tolerance dose for each OAR.

A more detailed group evaluation can also be done with the partial group plots (Structures Group Diagrams – SGD), where only the structures of that group are represented. As for the SPD and GPD, a partial group score complementing the graphical assessment is determined for each SGD.

For this study, all delineated structures were grouped according to their location and clinical importance into: PTV group (PTVs), Critical group (spinal cord and brainstem), Optics group (chiasm, optical nerves, retinas and lens), DigestOral group (parotids, oral cavity, oesophagus and larynx), Bone group (temporal mandibular joint, mandible and ear canals) and other group (brain, pituitary gland, thyroid and lungs). To each group a relative weight of 50%, 30%, 10%, 5%, 3.5% and 1.5%, respectively, was pre-assigned by the radiation oncologist. Within each group, the same weight was attributed each structure of that group. For detailed information, the reader is referred to Table S1 in the Supplementary material.

The score of each structure is determined considering the ratio between the clinical tolerance criteria and the planned dose. Thus, a value of one is expected if the dose for that structure is equal to the respective tolerance value. When a better organ sparing or target coverage is obtained, a score less than one will be obtained. Optimal scores will converge to the centre of the radar plot.

2.6. Statistical analysis

Statistical comparisons of the mean scores associated with each BAO algorithm and geometry sets were performed using IBM SPSS software, version 25. As the same set of patients is used to perform IMRT optimization applying the two BAO algorithms and different geometric settings, it was assumed that the samples were dependent. As the number of patients selected for this retrospective study is greater than 30, it was also considered that the samples follow a normal distribution. Statistically significant differences between the families of test were assessed with a randomized block design ANOVA test and, if applicable, a post-hoc multiple comparison test using the Tukey method. Single pair comparisons were statistically evaluated with the t-test. A level of significance of 5% was considered for all statistical tests.

2.7. Methodology used for the presentation of results

The results from the two BAO algorithms were structured in two subsections. In the first (Section 3.1), a beam angle distribution analysis was performed using circular diagrams for the coplanar geometries and 2D-maps for the non-coplanar situation. The mean angle incidences (calculated by sorting the beam angles calculated for each patient) and the associated standard deviation angles of each algorithm and the angles from the equidistant beam angle solution (d7) were also represented. For the coplanar geometries, the circular diagrams were composed by three concentric rings with an angle section resolution of 10° that were used to represent the relative frequencies of the beam angle distribution obtained for the two algorithms. The inner ring of the circular diagrams showed the beam angle distribution of the BAO with 5 beams, the middle ring corresponds to the optimization with 7 beams and in the external ring the 9 beams results were shown. Each ring was divided into eight regions, described in Table 1, commonly used in the clinical routine to label beam/patient orientations. For the non-coplanar plans, 2D-maps were used to perform the beam angle distribution analysis. A grid resolution of 10° was considered. The gantry angles axis (vertical) was divided in the same groups defined as for the coplanar case. The couch angles axis (horizontal) was grouped into five regions also included in Table 1.

The dosimetric performance of BAO optimizations is presented in Section 3.2 using SPIDERplan analysis. A mean global analysis of the plans dose distribution quality was performed using the global plan score and the partial group scores described above. Furthermore, an individual analysis for some patients with relevant global results was performed by presenting the GPD and SGDs of interest.

3. Results

3.1. Beam angle distribution

The frequency analysis of the beam angle distribution of algorithms *i* and *B* for 5, 7 and 9 beams is shown in Fig. 1 (coplanar setting) and
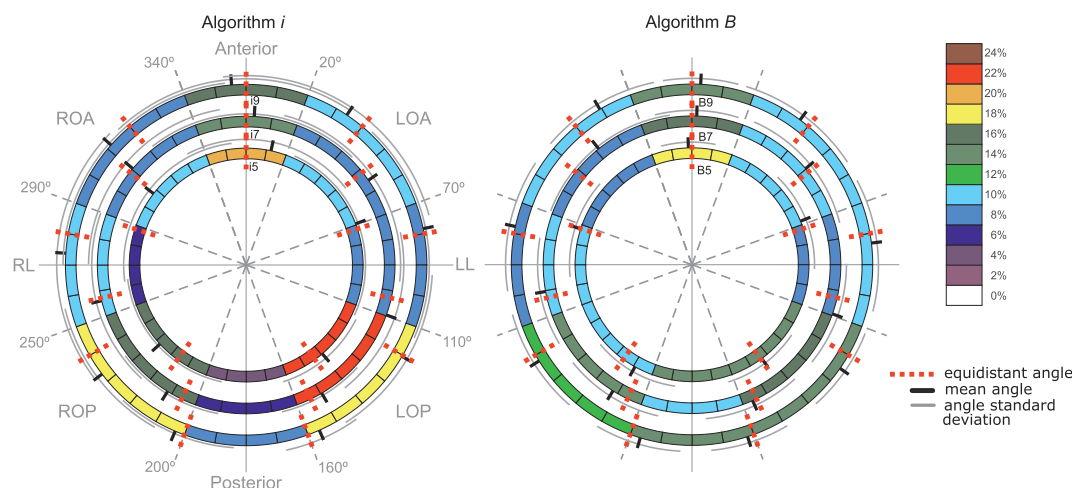
Fig. 1. Angular representation of the relative frequencies of the coplanar BAO of algorithms *i* and *B* for 5, 7 and 9 beams. The colour represents the relative frequencies obtained for each angle section: a hot colour is associated to a high relative frequency and a cold colour to a low relative frequency value. The mean angle incidences and the associated standard deviation angle values of each algorithm were represented with black solid pointers and grey solid arcs respectively. The red dash lines represent the beam angles of the equidistant beam angle solution (*d7*).

Fig. 2 (non-coplanar setting).

In Fig. 1, the beam angles for the equidistant beam angle solution (red dash lines) and the mean angle incidences (black solid pointers) with the associated standard deviation (grey solid arcs) are also represented in each circular beam diagram. The two coplanar BAO approaches presented distinct beam angular distribution patterns. In algorithm *i* (*i5*, *i7* and *i9*), based on an iterative BAO framework, the beam angular distribution across the regions was asymmetric with preferred regions very well defined as the LOP, the anterior or the ROP regions. The relative frequency values were comprehended between 4% and 22%. The higher relative frequency values, corresponding to the preferred irradiation directions, were the LOP region and the anterior region in *i5* set and also the ROP region in *i7* and *i9* sets. For algorithm *B* (*B5*, *B7* and *B9*), a more evenly angular distribution was obtained, with relative frequency values ranging between 8% and 18%. For all sets, the anterior, the posterior and the LOP regions presented the higher relative frequency values. For both algorithms, anterior-oblique and lateral orientations were not often selected as good irradiation directions regardless the number of beams used. The difference between the optimal mean angle and the correspondent equidistant beam was $0.8° \pm 34°$ for algorithm *i* and $1.5° \pm 19.9°$ for algorithm *B*.

In Fig. 2, for the non-coplanar BAO modality, the gantry angle distribution and the couch angle distributions are presented by a relative frequency 2D-map. The gantry angles axis and the couch angles axis were divided into regions of interest, referred in Table 1. For simplification each region, composed of a set of gantry and couch angles, will first be named with the gantry region followed by the couch region (for instance, posterior_CNC). In Fig. 2, the beams position for the equidistant coplanar beam plans are shown by the red dots, the individual beam incidences obtained by angular incidences by small black dots, the correspondent mean angle incidences by the large black dots and the associated standard deviation by the grey ellipses. Avoidance incidences, corresponding to potential collisions between gantry and couch, were represented by yellow grid squares. The two non-coplanar BAO algorithms presented again distinct beam distribution patterns. In algorithm *i*, most of the beams were uniformly distributed over the space, with relative frequencies ranging between 0% (white squares in Fig. 2) and 7% (cyan). Interestingly, the preferred irradiation directions selected by algorithm *i* where almost neglected by algorithm *B* where relative frequency values of less than 1% were obtained. In algorithm *B*, with relative frequency values ranging between 0% and 13%, it is possible to define a pattern for the beam's angular distribution. In fact, the non-coplanarity is almost confined to couch

angulation between −20° and 20°, corresponding to the CNC region. The remaining regions presented relative frequency values inferior to 2%.

The average beam incidences, and especially the standard deviation values, for both algorithms are quite different. Graphically, this can be perceived in Fig. 2 by the clear separation between the ellipses for algorithm *B* while for algorithm *i* the standard deviations ellipses overlap each other. Furthermore, the distance between the mean incident angles (large black dots) and the correspondent equidistant solution (red dots) are closer in algorithm *B* than in algorithm *i*.

3.2. SPIDERplan scores analysis

3.2.1. Global plan analysis

The values of the global plan score, implemented in SPIDERplan, for the d7 plans (equidistant beams) and coplanar and non-coplanar BAO of algorithms *B* and *i* for 5, 7 and 9 beams are shown in Fig. 3a. The mean SPIDERplan global plan scores ranged between 0.901 and 0.947. The lowest mean plan scores, i.e. the plans with better overall score performance, were obtained by *B9* non-coplanar *(B9nc)* and *B9* coplanar *(B9c)* sets. *i9c* plans attained the third best score, while *i9nc* set only achieved the eighth best score immediately below all plans using 7 beams. *B5c* and *B5nc* plans, respectively, obtained a better performance than *i7nc*. The highest mean global plan scores, and therefore the worst overall plan performances, were obtained with the *i5nc* and *i5c* sets.

The statistical analysis that was carried out allowed the identification of pairs of algorithms and beam angle configurations such that the generated treatment plans cannot be considered as being different from a statistical point of view. The results of the statistical analysis and the resulting p-value of each comparison led to seven subsets, grouping the algorithms that did not present statistically significant differences. It was thus possible to build sets, as presented by the horizontal axis of Fig. 3b, such that each set includes similar treatment planning results. As an example, subset 1 shown in Fig. 3b, with the lowest global plan scores, includes *B9nc*, *B9c*, *i9c*, *B7nc* and *B7c* meaning that the quality of these plans is statistically equivalent. Statistically significant differences were found between plans *B9nc* (positioned in subset 1) and plans *i9nc* (belonging to subsets 4 and 5). These results also show that BAO may bring no benefit to plan quality when compared to the equidistant beam angle solution – all those solutions that overlap the red solid line belonging to subsets 3, 4 and 5, like *i9c*, *i7nc*, *i9nc*, *B7nc* or *B7c*, do not significantly differ from it. However, better plan scores were obtained when the number of beams increased to 9 beams, as in *B9c* and *B9nc*
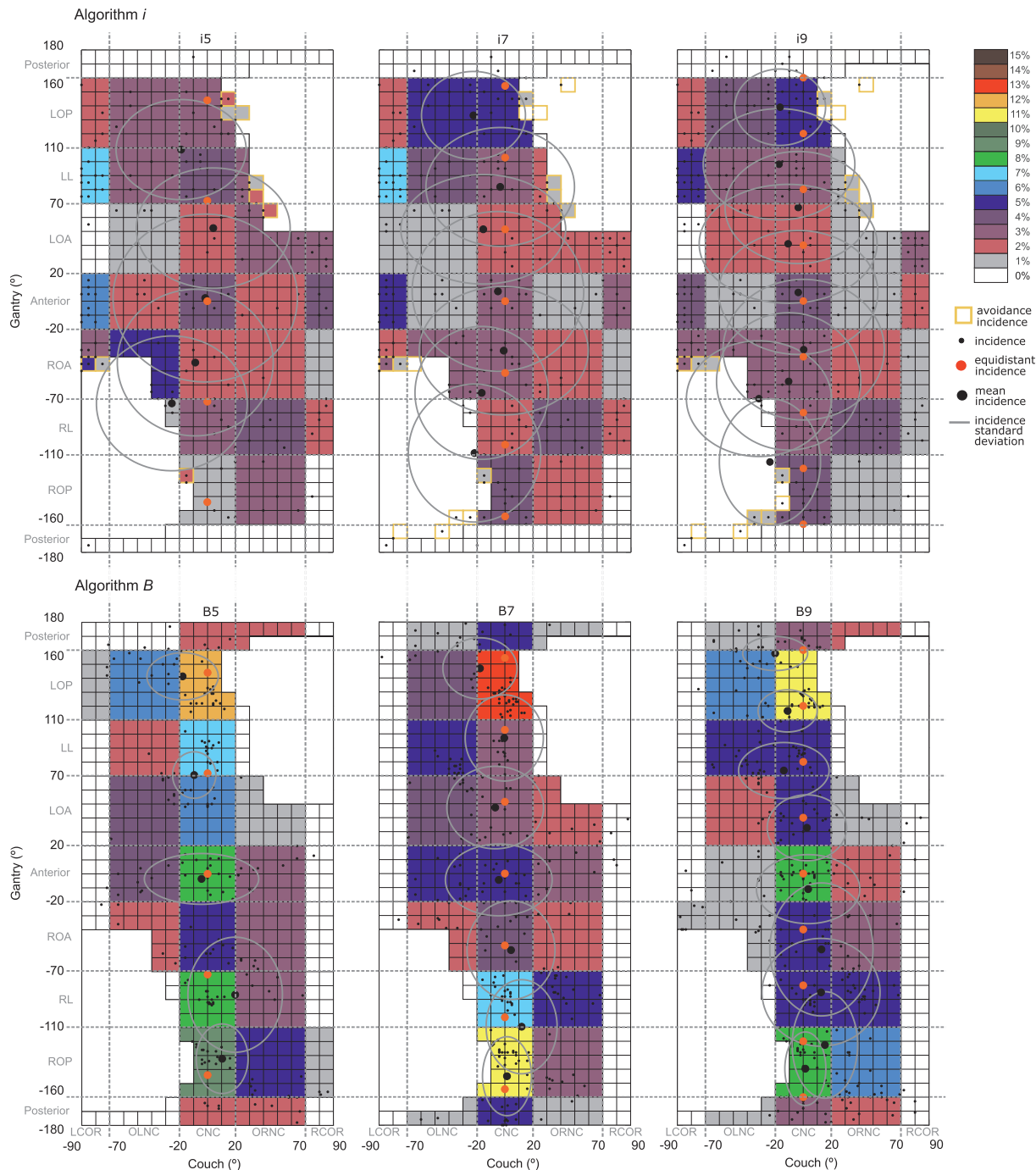
Fig. 2. 2D map representation of the relative frequencies of the non-coplanar BAO of algorithm *i* and *B* for 5, 7 and 9 beams. The gantry angles values are represented on the vertical axis and the couch angles on the horizontal axis. The colour represents the relative frequencies obtained for each angle section: a hot colour is associated to a high relative frequency. The mean angle incidences and the associated standard deviation angle values of each algorithm were represented with big black solid pointers and grey solid ellipses respectively. The small black solid pointers represent the angles incidence obtained with the BAO for all patients. The red solid points represent the beam angles values of the equidistant beam angle solution (*d7*).

(subset 1), compared to 7 beams (*i7nc or d7*). Also, while a statistically significant difference in plan quality was found between non-coplanar and coplanar plans using 9 beams whose positions were determined by algorithm *i*, for algorithm *B*, non-coplanarity brought no improvement in terms of plan quality. It is interesting to observe that, for algorithm *i* and 9 beams, the 9 beam coplanar plans were better than the non-co-planar ones.

The mean scores of coplanar and non-coplanar sets of algorithms *i* and *B* are compared in Fig. 4a and d, respectively. For algorithm *i*, the coplanar set had a lower mean score than the non-coplanar set

(p = 0.002) whereas for algorithm *B*, non-coplanar plans were statistically equivalent to coplanar ones (p = 0.960). Statistically significant differences were also found between non-coplanar plans optimized by algorithm *i* and *B* (p = 0.000), in favour of non-coplanar *B* plans, (Fig. 4e). The overall superior performance of algorithm *B* over algorithm *i* was statistically significant (p = 0.000), as demonstrated in Fig. 4f.

3.2.2. Group plan analysis

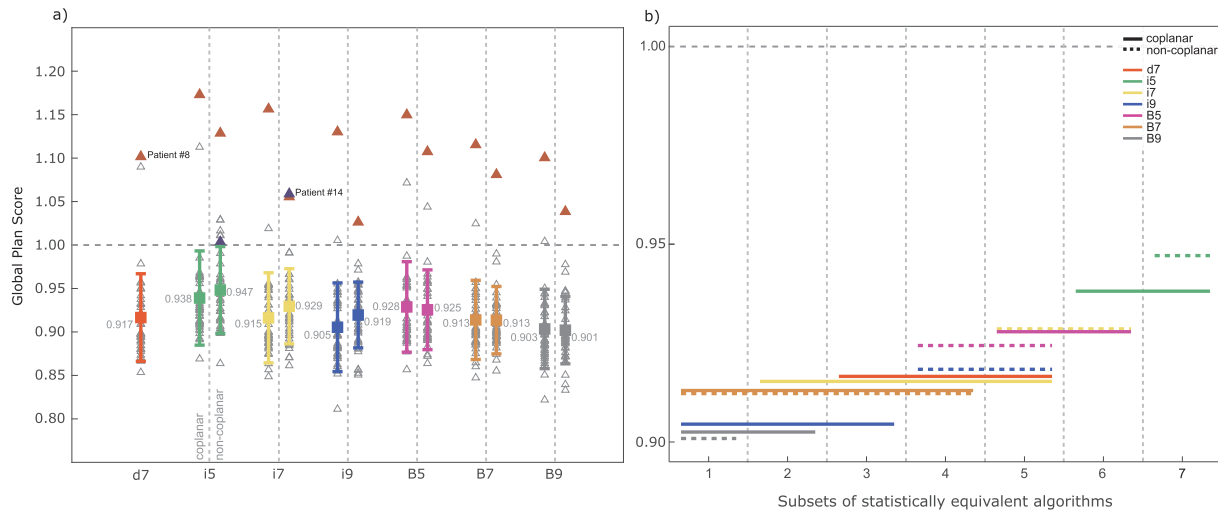The quality of the plans based on BAO algorithms *B* and *i* was

Fig. 3. a) SPIDERplan Global Plan scores, corresponding to all 40 clinical cases (triangles), for *d7* and for coplanar and non-coplanar BAO of algorithms i (coplanar plans: *i5c, i7c, i9c*, non-coplanar plans: *i5nc, i7nc* and *i9nc*) and B (*B5c, B7c, B9c, B5nc, B7nc* and *B9nc*). b) Homogenous subsets resulting from post-hoc multiple comparisons test using the Tukey method with a level of significance of 5% of the SPIDERplan global plan scores of each algorithm for coplanar and non-coplanar BAO.

assessed also using the information generated by SPIDERplan diagrams (Figs. S4–S8 in the Supplementary Material). Generally, the group score agreed with the analysis performed for the global plan score section. Almost all structure groups included in the optimization got mean scores below 1, meaning that the clinical criteria were on average accomplished. The exception was the DigestOral group, where for the parotids and for the oral cavity planned doses surpassed tolerance doses. Differences in the mean group scores between non-coplanar plans of algorithm *i* and the remaining plans and between 9 beams and 5 beams plans of algorithms *i* and *B* were also obtained for the Optics and the DigestOral groups, respectively.

The plans with higher number of beams and a non-coplanar geometry tend to lead to dose distributions with better quality, i.e. higher PTV coverage and higher OAR sparing. Some exceptions were found for the Optics and Bone groups. In the Optics group, the best scores were found for the coplanar beam geometries of algorithm *B* and the worst for the non-coplanar sets of algorithm *i*. For the Bone group, either the non-coplanar or the coplanar plans of algorithm *B* achieved the best performances, while the coplanar and the non-coplanar sets of algorithm *i* got the worst scores. Globally, algorithm *i* presented better scores for the two most important groups (PTV and Critical group), while algorithm *B* got the best scores for the remaining groups. However, the differences in plan quality for each structure group between the two algorithms were statistically significant just for the Optics and Bone groups, which included the OARs with the lowest clinical weight.

3.2.3. Individual patient analysis

The decision of which beam set-up should be used in a given patient must be well pondered and clinically assessed case by case. In Fig. 3a, two patients (patient #8 and #14) were identified with notorious high scores (worst plan quality). For patient #8 (red triangles in Fig. 3a), all plans obtained a global score superior to 1 and presented mean percent differences between the coplanar and the non-coplanar sets for algorithms *i* and *B* of −8% and −5%, respectively. For patient #14 (blue triangles in Fig. 3a), two plans exceeding the score threshold defined for SPIDERplan, presented an apparent contradictory score difference, wherein plan *i5nc* was better (lower score) than plan *i7nc*. The assessment of plan quality for patients #8 and #14 is presented in Figs. 5 and 6, using the GPD and the SGDs of SPIDERplan. Plans using equidistant beam angles (d7) and the plans with the best and worst global plan scores were selected for this individual analysis. One or more additional

sets were also considered to emphasize some results of interest observed in each patient.

For patient #8 (corresponding to Fig. S1 in the Supplementary material) the best global plan score was achieved by plan *i9nc* (global plan score of 1.026) and the worst global plan score, of 1.172, was obtained with plan *i5c*. An increase of 15% percent in plan quality of *i9nc* plan, when compared with i5c, was achieved when SPIDERplan global score is adopted as plan quality scoring metric. A percent difference of +11% was obtained between the global plan scores of i9nc and i9c. These differences highlight the potential benefits that can arise from angular optimization including non-coplanar beam angle incidences. The largest difference between the tolerance and the planned dose was obtained for the Optics group and the DigestOral group (Fig. 5). For the PTV group and in the Critical group some score values slightly higher than 1 were also obtained for some plans due to the proximity between the primary tumour mass, prescribed to 70 Gy, and the retinas, the optical nerves, the chiasm, the brainstem, the ears and the oral cavity. The increase in the number of beams with non-coplanar geometries led to important improvements in the OAR sparing, especially in the lens and the parotids but also in PTV coverage. Nevertheless, these improvements were not extensible to all structures where even worst results were obtained for the oral cavity when 9 non-coplanar beams were used.

For patient #14 (corresponding to Fig. S2 in the Supplementary material), *B9c* presented the best global plan score and *i7nc* the worst performance. A mean percent difference in the global score of −10% was achieved when coplanar and non-coplanar sets of algorithm *i* were compared (Fig. 6). For algorithm B, this mean percent difference was close to 0%, meaning that for this patient the non-coplanarity did not bring any advantage for algorithm B. Significant differences between the considered plans can be identified for the lens (Optics group), the left ear (Bone group) and for the left parotid (Digest Oral group). All structures but the right lens presented better scores for plans with higher number of beams and/or non-coplanar geometry. For the right lens, however, *i5nc* presented a better score than *i7nc*. This configures a situation where a larger number of beams did not bring improvements to the overall plan quality. Analysing the specific anatomy of patient #14, it is possible to observe that the primary mass PTV was well below the optical structures (chiasm, optical nerves, retinas and lens). This influenced the non-coplanar BAO process and probably the SPIDERplan analysis results, since some of the considered clinical criteria could probably have been relaxed.
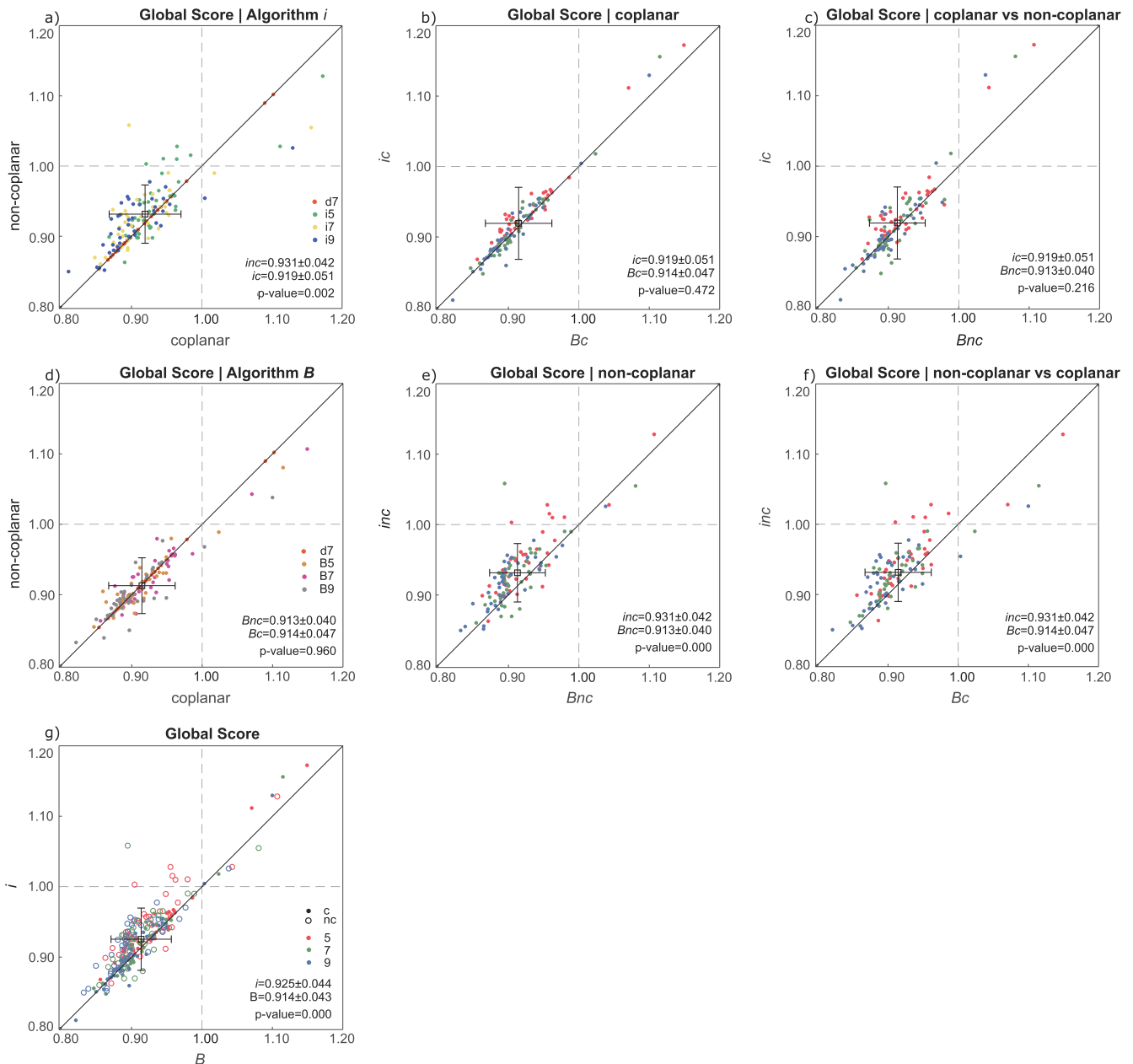
Fig. 4. Comparison between different plans optimized with algorithms *i* or *B* using coplanar or non-coplanar beams.

4. Discussion

In this work, the plans produced by two BAO algorithms, *i* and *B,* were evaluated and compared for NPC tumour cases. Forty clinical cases were retrospectively used to automatically determine the best incidences of 5, 7 and 9 beams plan sets with coplanar and non-coplanar geometries. The BAO and the FMO problems were addressed together by using a multicriterial IMRT optimization framework to guide the process. Algorithm *i* is based on a combinatorial iterative discrete search approach and is embedded in the multicriterial optimization framework. Algorithm *B* is based on a continuous space search using a pattern search method. It is also possible to consider the optimization of the number of beams. This can be done in a trivial way, by running different optimization procedures, each one for a different number of angles. The choice of the number of angles could also be incorporated in the optimization algorithm but given the complexity of the BAO the inclusion of one more degree of freedom could actually lead to worse results (since the size of the possible solutions space

would be enlarged). In the final optimization phase 240 plans with 27 associated structures were generated for each algorithm. Starting from the equidistant solution, BAO plans were considered, covering an expressive universe of 3640 beam incidences, 520 plans and 14,040 dosimetric structures statistics available to be analysed. The analysis of this large amount of data was done from two perspectives: the characterization of the beam angle distribution over the space search and the assessment of the quality of the dose distribution of the generated plans. To our knowledge, this is the first work that compares these two types of class methods for head and neck cancer taking into consideration all the clinical structures using subjacent clinical criteria. Furthermore, the graphical options *ad-hoc* constructed for this purpose, the circular diagrams for the coplanar case and the 2D-map for the non-coplanar one, enable an efficient global analysis that otherwise would be difficult to be performed.

The relative frequency patterns of the beam angle distribution for coplanar and non-coplanar beams geometries seemed to be conditioned by the optimization strategy followed by each algorithm. In algorithm *i,*
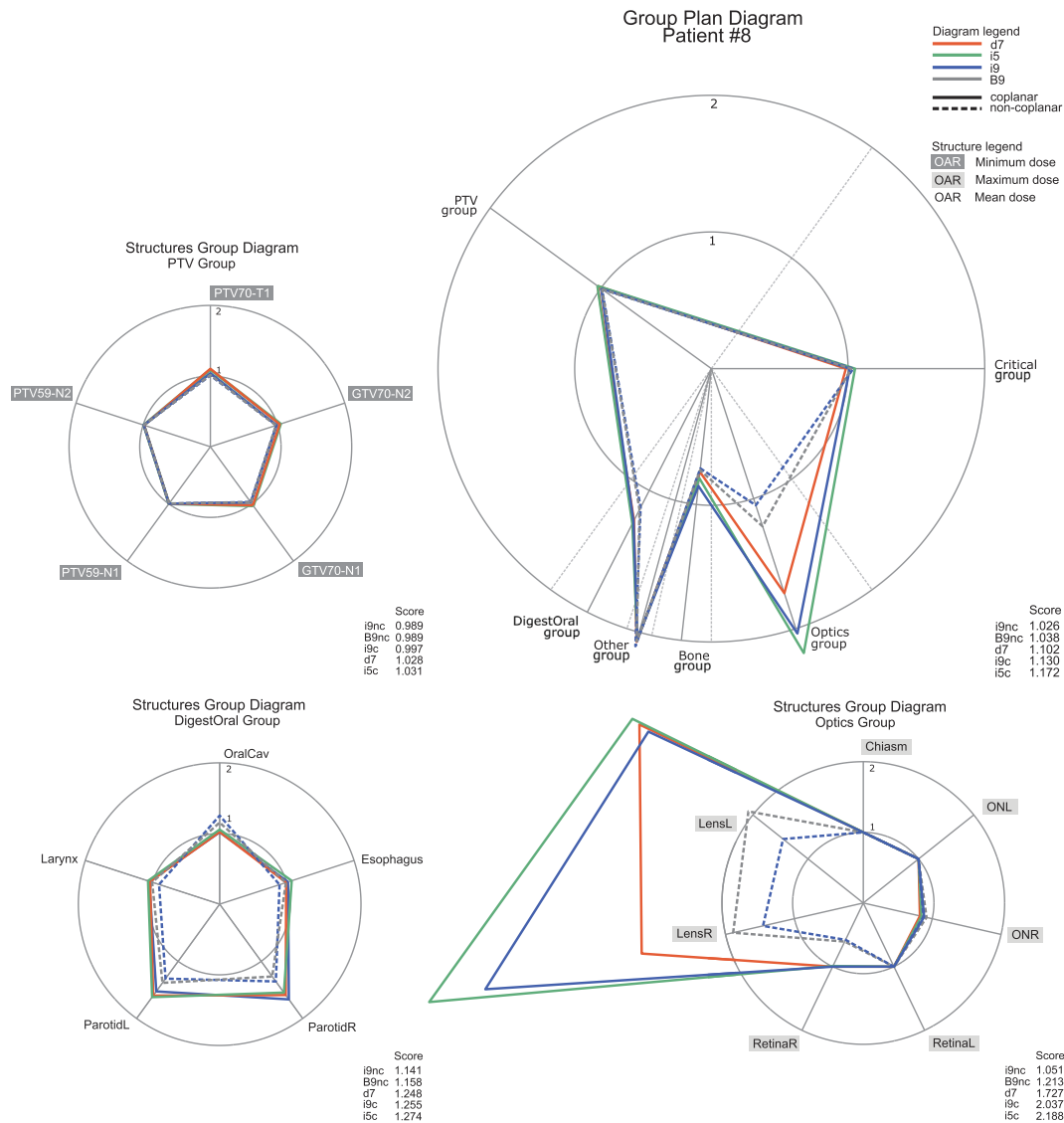
Fig. 5. SPIDERplan of patient number 8 and structures group diagram for PTV group, Optics group and DigestOral group.

beams with optimal orientation were iteratively added into the plan after being combined with the beams already selected in a discretized space search. For plans using coplanar beams, this cumulative beam adding methodology generated a non-uniform angle distribution pattern where it is possible to clearly identify favourite irradiation directions and regions of low preference. For non-coplanar beam plans this asymmetric beam distribution pattern with well-defined preferred incidences blurred into an almost uniform beam distribution pattern. This pattern change is a natural consequence of the selection of beam incidences over almost all the available space search. In algorithm *B*, the search for the best ensemble is initially done by considering a fixed number of incidences defined from the best equidistant coplanar angle set solution. This preliminary optimization is followed by the application of the pattern search method considering a continuous space search. Although the equidistant beam ensemble seems to be the most reasonable BAO starting point for this approach, the beam angle distribution maps presented patterns that may be strongly influenced by the initial solution. For coplanar geometries an almost uniform pattern, with low relative frequency values was patent in the circular diagram of frequencies. For the non-coplanar situation, the results follow the starting point option, being the non-coplanarity confined to modest deviations from zero couch position ($\pm 20°$). Comparing the mean incidences and the associated standard deviations obtained by the two

optimization algorithms, once again the optimization strategy of each of the algorithms is patent, leading algorithm *i* to more distributed incidence solutions and algorithm *B* proposing solutions closer to the initial equidistant case.

The quality assessment and comparison of the plans generated with BAO was performed using three types of approaches: a global plan analysis, a group plan analysis and an individual analysis of selected patients. This methodology was accomplished by the determination of SPIDERplan scores and an appropriate statistical analysis that conferred to the process the possibility to evaluate the dosimetric quality of the BAO with different levels of specificity. Increasing the number of beams brought improvements to the plan dose distribution. Nevertheless, for most cases only the comparison between 9 beam plans and 5 beam plans was significant statistical.

Algorithm *B* showed a more consistent behaviour and presented, by a moderate difference in score, a better performance than algorithm *i*. For the studied NPC tumour cases, on average, non-coplanarity brought no improvements to plan quality. For algorithm *B*, a better score was obtained when non-coplanar beams were compared with the corresponding coplanar solution but this difference was not statistically significant. These results confirmed some empirical impressions shared by many planners. In face of highly complex planning cases, beyond the manual tuning of the objectives and the associated weights, planners

Fig. 6. SPIDERplan of patient number 14 and structures group diagram for Optics group, DigestOral group and Other group.

usually try to play with the initial beam angle incidences or to increase the number of beams in order to improve the plans. The general assumption that plan quality improves when the number of beams increases is also supported by the results usually achieved with VMAT ("infinite" number of beam directions). Nevertheless, for the studied pathology, BAO seemed to bring only marginal improvements to the plan quality. A first explanation may be related with the anatomy of the NPC cases, where the PTVs with large extensions (up to 25 cm of height), the high number of critical structures along the field of irradiation and minimum exposure requirement for the remaining normal tissues may limit the optimization of the beam incidences. Another justification can be found in the use of the same wish-list for all patients and for both BAO approaches. The improvement that can be obtained by BAO is intrinsically linked to the FMO approach. Since the resources and time needed to find an optimal beam set are costly, if manual tuning is needed then the clinical utility of BAO must be seriously appraised. If BAO can be done in an automated way, then it will represent an added-value, since it can bring interesting improvements for some patients. In Erasmus-iCycle, the treatment planning procedure is almost automatic. The only think that is asked to the planner before the planning is to build and validate a wish-list that will guide the multi-criterial optimization process. For the NPC pathology, five test cases were used in the validation process. This initial configuration does not take long, and it has a reduced impact on the overall time spent with the optimization. More expressive score differences between the treatment planning sets could be achieved if the SPIDERplan score could be embedded in the BAO process as suggested by Rocha et al. [26]. As SPIDERplan methodology incorporates the radiation oncologist preferences, it could confer to the BAO process some proximity to the clinical aims and thus improve overall plan quality.

The overall weaker performance of algorithm *i*, when compared with algorithm *B*, is related with the results of the non-coplanar optimization in the Optics and in the Bone groups, since for the remaining groups these sets presented the best SPIDERplan scores. For the Bone group, although the non-coplanar optimization of algorithm *i* presented a better performance than the coplanar set of algorithm *i*, it was inferior to the coplanar optimization of algorithm *B*. For the Optics group, the results of the non-coplanar sets of algorithm *i* were by far the worst when compared with the remaining sets. Due to the anatomic localisation of the structures of these two groups and also to the optimization methodology subjacent to algorithm *i*, it was not expected that the non-coplanar optimization presented such results that were on average below the score tolerance but were worse than the remaining sets.

The weaker performance of non-coplanar solutions for algorithm *i* compared to coplanar plans is unexpected as the coplanar problem is a sub-solution of the non-coplanar problem. This might be a result of the complexity of BAO, a highly nonconvex problem with many local minima, particularly for complex tumour sites as NPC with a large

number of OARs. Obtaining the optimal solution is quite difficult, particularly for the non-coplanar case that explores a vaster search space. As it is not possible to guarantee that the optimal solution is found, and the algorithms do not perform an exhaustive search (which would be prohibitive both in terms of time and computational resources), it is possible that the best coplanar solution is not found when looking for a non-coplanar solution. A simple strategy to improve the performance of algorithm *B* would be to include the optimal solution of the coplanar BAO in the set of initial starting solutions. However, that strategy cannot be used for algorithm *i*, since it fixes one direction at each iteration. Whenever one direction is fixed, the search space is restricted in one dimension, meaning that there are solutions in the search space that cannot be visited in the subsequent iterations. The algorithm may be prevented from exploring better regions and the probability of getting trapped in local minima increases.

An important application of non-coplanar BAO is its importance in the calculation of non-coplanar intensity-modulated arc trajectories in VMAT. In fact, some of the arc trajectory algorithms are two-step approaches where, in the first step, non-coplanar BAO is performed using previously tested BAO algorithms and, in a second step, an arc trajectory optimization is performed using the beam directions found in the first step as anchor points [10]. The fact that algorithm *B* obtain solutions for a more limited range of couch angles, with a superior quality to the solutions of algorithm *i*, might represent a competitive advantage for its use in the calculation of non-coplanar trajectories in VMAT planning.

5. Conclusions

In this work the beam angle optimization IMRT was addressed using forty head-and-neck cancer clinical cases. Two algorithms, based on a combinatorial iterative (algorithm *i*) and on a continuous exploration of the space search (algorithm *B*) approaches, were assessed and compared for coplanar and non-coplanar beam geometries. A graphical method for plan quality assessment and comparison, named SPIDERplan, was used. The two algorithms were assessed through the analysis of the beam angle distribution and of the plan quality. The great amount of generated data was managed through graphical plots that enabled efficient global analysis and comparisons. Algorithm *i* for coplanar optimization presented a less uniform angle distribution pattern whereas for non-coplanar optimization the beam distribution pattern was almost uniform. For algorithm *B*, both beam angles geometries options were strongly influenced by the starting equidistant solution. Concerning assessment and comparison of plan quality for BAO algorithms, slightly better score performance was achieved by algorithm *B,* when compared to algorithm *i*. For algorithm *B*, coplanar and non-coplanar beam angle geometries were statistically equivalent, while for algorithm *i*, non-coplanar solutions were statistically worse than the correspondent coplanar due to the optimization strategy followed by this algorithm. Nevertheless, for specific patients strong benefits were obtained, and angle optimization proved to be valuable.

The results of the present study can potentially be applied in VMAT planning through the calculation of non-coplanar modulated arc trajectories.

Acknowledgments

No potential conflict of interest nor any financial disclosures must be declared.

Appendix A. Supplementary data

Supplementary data to this article can be found online at https://doi.org/10.1016/j.ejmp.2019.07.012.

References

[1] ICRU. International Commission on radiation units and measurements. Prescribing, recording, and reporting photon-beam intensity-modulated radiation therapy (IMRT). ICRU Report 83. J ICRU 2010;10(1):1–106. https://doi.org/10.1093/jicru/10.1.Report83.

[2] Zhang Y, Merritt M. Dose–volume-based IMRT fluence optimization: a fast least-squares approach with differentiability. Linear Algebr Appl 2008;428:1365–87. https://doi.org/10.1016/j.laa.2007.09.037.

[3] Spirou SV, Chui CS. A gradient inverse planning algorithm with dose–volume constraints. Med Phys 1998;25(3):321–33. https://doi.org/10.1118/1.598202.

[4] Webb S. Optimization of conformal radiotherapy dose distributions by simulated annealing. Phys Med Biol 1989;34(10):1349–70. https://doi.org/10.1088/0031-9155/34/10/002.

[5] Thieke C, Küfer KH, Monz M, Scherrer A, Alonso F, Oelfke U, et al. A new concept for interactive radiotherapy planning with multicriteria optimization: first clinical evaluation. Radiother Oncol 2007;85(2):292–8. https://doi.org/10.1016/j.radonc.2007.06.020.

[6] Miettinen K. Nonlinear Multiobjective Optimization New York: Springer US; 1998. https://doi.org/10.1007/978-1-4615-5563-6.

[7] Branke J, Deb K, Miettinen K, Słowiński R. Multiobjective optimization. Interactive and Evolutionary Approaches 1st ed.New York: Springer-Verlag Berlin Heidelberg; 2008. https://doi.org/10.1007/978-3-540-88908-3.

[8] Das SK, Marks LB. Selection of coplanar or noncoplanar beams using three-dimensional optimization based on maximum beam separation and minimized non-target irradiation. Int J Radiat Oncol Biol Phys 1997;38(3):643–55. https://doi.org/10.1016/S0360-3016(97)89489-8.

[9] Rocha H, Dias J, Ventura T, Ferreira B, Lopes MC. A derivative-free multistart framework for an automated noncoplanar beam angle optimization in IMRT. Med Phys 2016;43(10):5514–26. https://doi.org/10.1118/1.4962477.

[10] Papp D, Bortfeld T, Unkelbach J. A modular approach to intensity-modulated arc therapy optimization with noncoplanar trajectories. Phys Med Biol 2015;60(13):5179–98. https://doi.org/10.1088/0031-9155/60/13/5179.

[11] Bortfeld T, Schlegel W. Optimization of beam orientations in radiation therapy: some theoretical considerations. Phys Med Biol 1993;38(2):291–304. https://doi.org/10.1088/0031-9155/38/2/006.

[12] Ehrgott M, Holder A, Reese J. Beam selection in radiotherapy design. Linear Algebra Appl 2008;428(5):1272–312. https://doi.org/10.1016/j.laa.2007.05.039.

[13] Craft D. Local beam angle optimization with linear programming and gradient search. Phys Med Biol 2007;52(7):127–35. https://doi.org/10.1088/0031-9155/52/7/N02.

[14] Stein J, Mohan R, Wang XH, Bortfeld T, Wu Q, Preiser K, et al. Number and orientation of beams in intensity-modulated radiation treatments. Med Phys 1997;24(2):149–60. https://doi.org/10.1118/1.597923.

[15] Pugachev A, Lei X. Pseudo beam's-eye-view as applied to beam orientation selection in intensity-modulated radiation therapy. Int J Radiat Oncol Biol Phys 2001;51(5):1361–70. https://doi.org/10.1016/S0360-3016(01)01736-9.

[16] Dias J, Rocha H, Ferreira BC, Lopes MC. Simulated annealing applied to IMRT beam angle optimization: a computational study. Phys Med 2015;31(7):747–56. https://doi.org/10.1016/j.ejmp.2015.03.005.

[17] Dias J, Rocha H, Ferreira BC, Lopes MC. A genetic algorithm with neural network fitness function evaluation for IMRT beam angle optimization. Cent Eur J Oper Res 2014;22(3):431–55. https://doi.org/10.1007/s10100-013-0289-4.

[18] Aleman DM, Kumar A, Ahuja RK, Romeijn HE, Dempsey JF. Neighborhood search approaches to beam orientation optimization in intensity modulated radiation therapy treatment planning. J Global Optim 2008;42(4):587–607. https://doi.org/10.1007/s10898-008-9286-x.

[19] Lim GJ, Cao W. A two-phase method for selecting IMRT treatment beam angles: Branch-and-Prune and local neighborhood search. Eur J Oper Res 2012;217(3):609–18. https://doi.org/10.1016/j.ejor.2011.09.038.

[20] Bertsimas D, Cacchiani V, Craft D, Nohadani O. A hybrid approach to beam angle optimization in intensity-modulated radiation therapy. Comput Oper Res 2013;40(9):2187–97. https://doi.org/10.1016/j.cor.2012.06.009.

[21] Sultan ASA. Optimization of beam orientations in intensity modulated radiation therapy planning PhD Thesis Germany: Department of Mathematics, Technical University of Kaiserslautern; 2006.

[22] Lim GJ, Choi J, Mohan R. Iterative solution methods for beam angle and fluence map optimization in intensity modulated radiation therapy planning. OR Spectrum 2008;30(2):289–309. https://doi.org/10.1007/s00291-007-0096-1.

[23] Breedveld S, Storchi P, Voet P, Heijmen B. iCycle: integrated, multi-criterial beam angle and profile optimization for generation of coplanar and non-coplanar IMRT plans. Med Phys 2012;39(2):951–63. https://doi.org/10.1118/1.3676689.

[24] Bangert M, Unkelbach J. Accelerated iterative beam angle selection in IMRT. Med Phys 2016;43(3):1073–82. https://doi.org/10.1118/1.4940350.

[25] Rocha H, Dias J, Ferreira BC, Lopes MC. Beam angle optimization for intensity-

modulated radiation therapy using a guided pattern search method. Phys Med Biol 2013;58(9):2939–53. https://doi.org/10.1088/0031-9155/58/9/2939.

[26] Rocha H, Dias JM, Ventura T, Ferreira B, Lopes M. Beam angle optimization in IMRT: are we really optimizing what matters? Intl. Trans in Op Res 2019;26(3):908–28. https://doi.org/10.1111/itor.12587.

[27] Breedveld S, Storchi P, Keijzer M, Heemink A, Heijmen B. A novel approach to multi-criteria inverse planning for IMRT. Phys Med Biol 2007;52(20):6339–53. https://doi.org/10.1088/0031-9155/52/20/016.

[28] Ventura T, Lopes MC, Ferreira BC, Khouri L. SPIDERplan: a tool to support decision-making in radiation therapy treatment plan assessment. Rep Pract Oncol Radiother 2016;21(6):508–16. https://doi.org/10.1016/j.rpor.2016.07.002.

[29] Breedveld S, Storchi P, Heijmen B. The equivalence of multi-criteria methods for radiotherapy plan optimization. Phys Med Biol 2009;54(23):7199–209. https://doi.org/10.1088/0031-9155/54/23/011.

[30] Custódio AL, Rocha H, Vicente LN. Incorporating minimum Frobenius norm models in direct search. Comput Optim Appl 2010;46:265–78. https://doi.org/10.1007/s10589-009-9283-0.